

# Evaluation of gear power losses from experimental test data and analytical methods

**B. Łazarz\*, G. Wojnar\*\*, H. Madej\*\*\*, P. Czech\*\*\*\***

\*The Silesian University of Technology, Krasińskiego 8, 40-019 Katowice, Poland, E-mail: Boguslaw.Lazarz@polsl.pl

\*\*The Silesian University of Technology, Krasińskiego 8, 40-019 Katowice, Poland, E-mail: Grzegorz.Wojnar@polsl.pl

\*\*\*The Silesian University of Technology, Krasińskiego 8, 40-019 Katowice, Poland, E-mail: Henryk.Madej@polsl.pl

\*\*\*\*The Silesian University of Technology, Krasińskiego 8, 40-019 Katowice, Poland, E-mail: Piotr.Czech@polsl.pl

## 1. Introduction

Toothed gears are widely used in the systems transmitting mechanical power of transport machine. They are also used in both simple everyday articles and very complex devices produced usually in single units. Since it is impossible to describe real phenomena or processes accurately, the practice is to adopt a model corresponding with reality to some limited extent and providing approximate (qualitatively and quantitatively) results comparable with observation and test results [1]. This comparison helps to assess usability of the model in solving given constructional problem.

The adapted dynamic model of a gear, with a proper structure and respecting all significant factors influencing meshing teeth loads and their distribution may be a useful tool in the design of toothed gears characterised by long lifetime [2].

For the above reasons, lots of scientific research centres around the world have developed more and more perfect dynamic models of toothed gears and complete drive systems with gears [3]. Due to difficulties arising in solving differential equations of motion these models were characterised by low number of degrees of freedom at first. Over the years the models have evolved in two following directions:

- accurate analysis of gear isolated from the drive system; the only causes of dynamic loading are internal, and the external load is constant;
- investigation of dynamic properties of complete drive systems consisting of a motor, toothed gear, principal process machine, shafts, couplings and intermediate elements; simplified dynamic models of meshing are used.

From the viewpoint of the authors of this paper's, the most important models representing the first line of investigation are: A. Kovalev's model [4, 5], J. Bollinger and M. Bosch's model [6], dynamic translational-rotational model with parametric excitations from variable mesh stiffness and tooth sliding friction moments [7], H. Rettig's model [8] and L. Müller's model [9].

Examples of models consisting of a motor, toothed gear, principal process machine, shafts, couplings and intermediate elements with simplified meshing operation modelling are: W. Nadolski's models [10, 11], F. Pfeiffer's model [12] and Litak and Friswell model [13].

In the view of rapid and extensive evolution of computer hardware and accompanying increase in computational power, nowadays it is possible to obtain fast calculation results from models taking into consideration dy-

namics of the complete drive system and describing effects occurring during meshing with relative accuracy. Examples of such models are:

- quoted in [14-18];
- and the new model presented in [19] possesses 34 degrees of freedom as opposed to 16 degrees of freedom in the previous model [20]. The extra 18 degrees of freedom are due to the inclusion of the five degrees of freedom in bearing model, and to the fact that translational degrees of freedom (DOF) are now considered both along the line of action (LOA) and in the direction perpendicular to LOA.

Apart from dynamic models of drive systems with single-stage gear and parallel or crossing axes, the following models are also in existence:

- two-stage gearing system with six torsional degrees of freedom [21];
- model shown in [22], which makes it possible to simulate epicyclic gear operation;
- model shown in [23], which makes it possible to simulate operation of wave gear coupled with a dc motor.

It is not possible to cite here all researchers working on toothed gear modelling. Extensive surveys of gears dynamic models and recapitulations of state-of-the-art may be found in references [15, 24, 25].

## 2. Model of a gear in power transmission system

The model obtained in Matlab-Simulink takes into account the interactions of different internal and external factors that occur during gear operation in power transmission system [15]. Diagram of the dynamic model is presented in Fig. 1. The model proposes a power transmission system that consists of propulsion engine, single-stage spur gear, process machine, and couplings connecting the shafts. The global coordinate system was designed in such a way that the  $x$ -axis coincides with gears shaft directions, the direction of the  $y$ -axis is in accordance with the axial force in the mesh, while the  $z$ -axis is in agreement with the contact force in the mesh. In this model, the gear and pinion are treated as rigid solids with known moments of inertia. The masses of remaining gear elements are reduced to the masses concentrated in the bearing centres. Additionally, it is assumed that these masses have nonzero moments of inertia in the direction of the rotation axis of the bearings.

The model may also be used for virtual reduction of the designed or selected gear in the power transmission system. Basing on the model, it is also possible to simulate

gear operation taking into consideration wear or damage of its elements. The model makes it possible to analyse impact of active surface wear and gear local faults on the form and level of the vibro-acoustic signal.

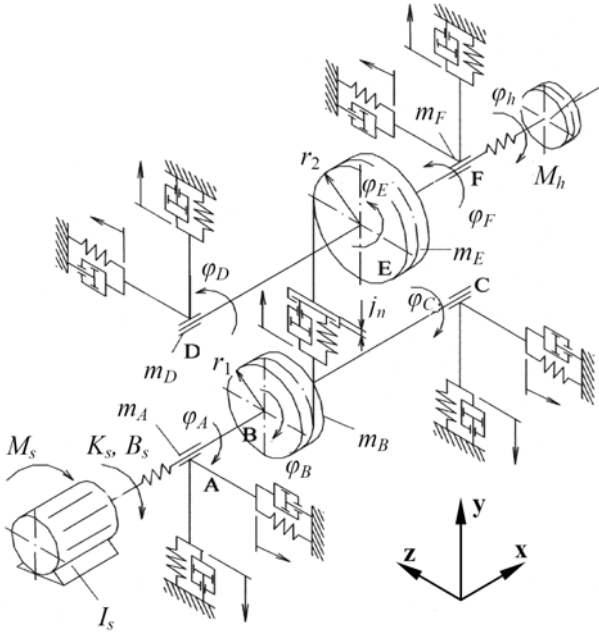


Fig. 1 Model of gear in transmission system

The global coordinate system shown in Fig. 1 is constructed in the following way:

- $x$ -axis coincides with gearbox shaft directions;
- direction of the  $y$ -axis is in agreement with the line of action;
- direction of  $z$ -axis is perpendicular to both  $x$  and  $y$  axes.

It has been assumed that each of the solids (A, B, C, D, E, F) has six degrees of freedom; in case of solid A and its displacement along  $x$ ,  $y$  and  $z$  axes these degrees are indicated with  $u_A$ ,  $v_A$ ,  $w_A$ , respectively, while in case of its rotation round  $x$ ,  $y$  and  $z$  axes these degrees are indicated with  $\varphi_{xA}$ ,  $\varphi_{yA}$ ,  $\varphi_{zA}$ , respectively. Moments of inertia and deviation of the solid have been calculated with respect to central axes parallel to the global coordinate system axes and denoted as  $I_x^A$ ,  $I_y^A$ ,  $I_z^A$ ,  $I_{xy}^A$ ,  $I_{xz}^A$ ,  $I_{yz}^A$ . In consideration of the great number of degrees of freedom of the model, the rotations around axes  $y$  and  $z$  have been neglected for A, C, D and F bearings. The motion equations of the analysed model have been determined from the following general relationship

$$\frac{d}{dt} \left( \frac{\partial E_K}{\partial \dot{q}_i} \right) - \frac{\partial E_K}{\partial q_i} + \frac{\partial V}{\partial q_i} = \hat{Q}_i - \frac{\partial D}{\partial \dot{q}_i}, \quad i=1, \dots, n_{ss} \quad (1)$$

where  $E_K$  is kinetic energy;  $V$  is potential energy;  $D$  is dissipation energy;  $\hat{Q}_i$  are generalised forces;  $q_i$  are generalised co-ordinates;  $n_{ss}$  is the number of degrees of freedom.

It has been assumed that for a designed gear the bearings are located as close as possible to the toothed wheels. In such a case, the distance AC and DF is relatively small, and bending rigidity of the shafts is high. Shaft torsional rigidity is much higher than torsional rigid-

ity of the couplings and the result is that ends of AC and DF shafts (Fig. 1) may only execute moves dependent on pinion B and wheel E displacements, respectively. The following wheel displacements are therefore left in the system:  $u_B, v_B, w_B, \varphi_{xB}, \varphi_{yB}, \varphi_{zB}$  and  $u_E, v_E, w_E, \varphi_{xE}, \varphi_{yE}, \varphi_{zE}$  as well as angles  $\varphi$  and  $\varphi_h$ .

In the next phase motion in the  $z$ -axis direction has been neglected as well as the possibility of rotation around  $y$ -axis, it has also been assumed that wheels moments of deviation are nil:  $I_{xy}^B = I_{xz}^B = I_{yz}^B = 0$  and  $I_{xy}^E = I_{xz}^E = I_{yz}^E = 0$ .

So, the equations of motion take the following form [15]

$$I_s \ddot{\varphi} - B_s (\dot{\varphi}_{xB} - \dot{\varphi}) - K_s (\varphi_{xB} - \varphi) = M_s(t) \quad (2)$$

$$(m_A + m_B + m_C) \ddot{u}_B + (b_{xA} + b_{xB} + b_{xC}) \dot{u}_B + (c_{xA} + c_{xC}) u_B = -F_b \quad (3)$$

$$m_A (\ddot{v}_B + l_{AB} \ddot{\varphi}_{zB}) + m_B \ddot{v}_B + m_C (\ddot{v}_B - l_{BC} \ddot{\varphi}_{zB}) + b_{yA} (\dot{v}_B + l_{AB} \dot{\varphi}_{zB}) + b_{yB} \dot{v}_B + b_{yC} (\dot{v}_B - l_{BC} \dot{\varphi}_{zB}) + c_{yA} (v_B + l_{AB} \varphi_{zB}) + c_{yC} (v_B - l_{BC} \varphi_{zB}) = F_n \quad (4)$$

$$(I_x^A + I_x^B + I_x^C) \ddot{\varphi}_{xB} + (B_{xA} + B_{xB} + B_{xC}) \dot{\varphi}_{xB} + B_s (\dot{\varphi}_{xB} - \dot{\varphi}) + K_s (\varphi_{xB} - \varphi) = (F_n \cos \alpha_w - F_t \sin \alpha_w) r_{w1} - M_{RA} - M_{RC} \quad (5)$$

$$m_A (\ddot{v}_B + l_{AB} \ddot{\varphi}_{zB}) l_{AB} + I_z^B \ddot{\varphi}_{zB} + m_C (\ddot{v}_B - l_{BC} \ddot{\varphi}_{zB}) (-l_{BC}) + b_{yA} (\dot{v}_B + l_{AB} \dot{\varphi}_{zB}) l_{AB} + b_{yC} (\dot{v}_B - l_{BC} \dot{\varphi}_{zB}) (-l_{BC}) + c_{yA} (v_B + l_{AB} \varphi_{zB}) l_{AB} + c_{yC} (v_B - l_{BC} \varphi_{zB}) (-l_{BC}) = -F_b r_{w1} \sin \alpha_w \quad (6)$$

$$(m_D + m_E + m_F) \ddot{u}_E + (b_{xD} + b_{xE} + b_{xF}) \dot{u}_E + (c_{xD} + c_{xF}) u_E = F_b \quad (7)$$

$$m_D (\ddot{v}_E + l_{DE} \ddot{\varphi}_{zE}) + m_E \ddot{v}_E + m_F (\ddot{v}_E - l_{EF} \ddot{\varphi}_{zE}) + b_{yD} (\dot{v}_E + l_{DE} \dot{\varphi}_{zE}) + b_{yE} \dot{v}_E + b_{yF} (\dot{v}_E - l_{EF} \dot{\varphi}_{zE}) + c_{yD} (v_E + l_{DE} \varphi_{zE}) + c_{yF} (v_E - l_{EF} \varphi_{zE}) = -F_n \quad (8)$$

$$(I_x^D + I_x^E + I_x^F) \ddot{\varphi}_{xE} + (B_{xD} + B_{xE} + B_{xF}) \dot{\varphi}_{xE} + B_h (\dot{\varphi}_{xE} - \dot{\varphi}_h) + K_s (\varphi_{xE} - \varphi_h) = -(F_n \cos \alpha_w - F_t \sin \alpha_w) r_{w2} - M_{RD} - M_{RF} \quad (9)$$

$$I_h \ddot{\varphi}_h - B_h (\dot{\varphi}_{xE} - \dot{\varphi}_h) - K_h (\varphi_{xE} - \varphi_h) = -M_h(t) \quad (10)$$

$$m_D (\ddot{v}_E + l_{DE} \ddot{\varphi}_{zE}) l_{DE} + I_z^E \ddot{\varphi}_{zE} + m_F (\ddot{v}_E - l_{EF} \ddot{\varphi}_{zE}) (-l_{EF}) + b_{yD} (\dot{v}_E + l_{DE} \dot{\varphi}_{zE}) + b_{yF} (\dot{v}_E - l_{EF} \dot{\varphi}_{zE}) (-l_{EF}) + c_{yD} (v_E + l_{DE} \varphi_{zE}) l_{DE} + c_{yF} (v_E - l_{EF} \varphi_{zE}) (-l_{EF}) = -F_b r_{w2} \sin \alpha_w \quad (11)$$

## 2.1. Model of the drive motor

Synchronous and asynchronous electric motors are universally used for machine and device drives. Many different advanced models of electric motors are known. Ready-made computer software simulating operation of asynchronous motors is available (e.g. model included in

Simulink programme [26]). From the point of view of toothed gear dynamics these models are too complex, since they compute lots of electrical parameters useless in the toothed gears modelling, and this lengthens computational time. That is why asynchronous motor model using torque-speed characteristic of the motor and rotor's moment of inertia has been used in current research.

$$M_n = M_s(n) - I_s \ddot{\phi} \quad (12)$$

and

$$n = \frac{30}{\pi} \dot{\phi} \quad (13)$$

where  $M_n$  is motor's driving torque, Nm;  $M_s(n)$  is torque of the motor calculated from torque-speed characteristic (Fig. 2);  $n$  is rotational speed of the shaft, RPM;  $I_s$  is moment of inertia of the rotor,  $\text{kg}\cdot\text{m}^2$ ;  $\ddot{\phi}$  is angular acceleration of the motor shaft,  $\text{rad/s}^2$ ;  $\dot{\phi}$  is angular speed of the motor shaft,  $\text{rad/s}$ .

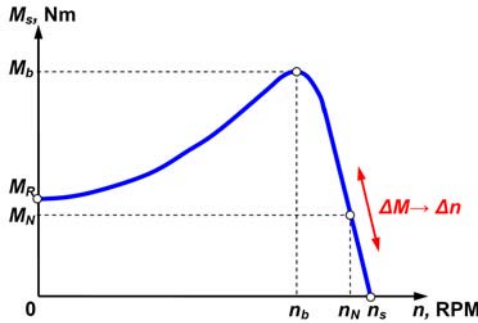


Fig. 2 Torque-speed characteristic of asynchronous motor

This model takes into account mesh vibration suppression, variable mesh stiffness, stiffness and suppression of gear bearings, as well as nonlinearity of phenomena occurring as an effect of backlashes in manufacturing deviations in the kinematic pairs. The simulation program, which is divided into two parts, allows such input data as:

- parameters of the gear and elements of the power transmission system;
- characteristics of electric motor.

The following (among others) constants and quantities that do not change during the simulation are calculated basing on the input data: mesh stiffness, moments of inertia, and masses of the transmission system elements. The second part of the simulation program is run in the Simulink environment, which makes it possible to construct block diagrams of equations in an uncomplicated way. The dynamic simulation model allows us to determine displacements, velocities and accelerations of pinion and gear shaft vibrations, as well as forces in bearing hubs.

## 2.2. Meshing stiffness

The loaded tooth bends and the deflection depends on the point of load application, material properties and tooth shape. Regardless of tooth shape, both surfaces at the place of contact become flattened, and at the same time the toothed ring becomes strained near the tooth root. Since both teeth bend, become flattened and strained at the

same time, the teeth pair stiffness changes along the line of action  $E_1E_2$  (Fig. 3) [9, 16]. Lots of authors assume that during stiffness calculations, the strain in the region of meshing teeth, the teeth bends and toothed rings strains must be considered (the teeth are modelled as beams) [9]. This problem may also be solved with the help of Finite Element Method (FEM) [16, 17] or Boundary Element Method (BEM) [27] (Fig. 3). In order to calculate meshing stiffness Boundary Element Method has been employed. We have used the software based on Müller's method and created in Department of Automotive Vehicle Construction, Faculty of Transport, of the Silesian University of Technology [9]. This software makes it possible to formulate profiles of any tooth of wheels with internal or external teeth and to carry out state of stress analysis.

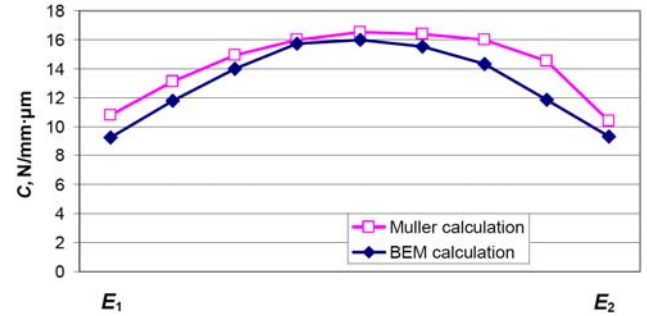


Fig. 3 Comparison of meshing stiffness calculated with Müller method and BEM method (stiffness as per 1 mm of face width)

## 2.3. Bearing stiffness

In consideration of their properties, the rolling bearings are widely used in toothed gears. The choice of method used to calculate bearing stiffness has been discussed in [15]. Finally, the method described in reference [28] has been adopted. In case of standard ball bearings the radial displacement  $\delta_r$ , mm may be calculated from the equation

$$\delta_r = \frac{4.4 \cdot 10^{-4} Q_t^{2/3}}{d_k^{1/3} \cos \alpha_l} \quad (14)$$

where  $Q_t$  is load of rolling element, N;  $d_k$  is diameter of the ball element, mm;  $\alpha_l$  is bearing contact angle, °.

The variable bearing stiffness may be expressed as

$$c_{loz} = \frac{Q_t(t)}{\delta_r(Q_t(t))} \quad (15)$$

The application of this model of drive system with toothed gear in design and dynamic analysis requires verification of model's parameters. One of the parameters is power loss coefficient, which influences the gear efficiency. Determination of this coefficient's value is important, since it exerts significant influence on both simulation results and their qualitative and quantitative conformity with experimental tests carried out on actual object.

## 3. Toothed gear efficiency

The power losses of toothed gears are due mainly

to: friction and vibration damping in the oil layer between the teeth, oil splashing and bearing friction. Since the energy dissipation reasons are varied and of random character, the accurate mathematical description of these forces is rather difficult.

### 3.1. Power losses due to oil splashing

The losses caused by oil splashing have been determined in accordance with reference [29]. For one toothed wheel immersed in oil to the depth  $H$  the dimensionless coefficient of oil splashing losses  $s_o$  is calculated with the help of the following empirical relationships (it must be noted that these relationships are true for a given unit system):

- for  $H \leq 25$  mm and  $v \geq 10$  m/s

$$s_o = \frac{vbH\sqrt{v}}{7 \cdot 10^5 N_1} \quad (16)$$

- for  $H \leq 25$  mm and  $v < 10$  m/s, and also for  $25 < H < 50$  mm irrespective of speed, loss coefficient is equal to

$$s_o = \frac{v^{1.5}bH\sqrt{v}}{20 \cdot 10^5 N_1} \quad (17)$$

- for  $H > 50$  mm irrespective of speed

$$s_o = \frac{v^2bH\sqrt{v}}{70 \cdot 10^5 N_1} \quad (18)$$

where  $v$  is circumferential speed, m/s;  $b$  is circle width, mm;  $H$  is depth of immersion, mm;  $N_1$  is transmitted power, kW;  $v$  is oil kinematic viscosity,  $\text{mm}^2/\text{s}$ . The absolute value of power loss due to oil splashing is equal to

$$\Delta N_o = s_o N_1 \quad (19)$$

When relationships 16-19 are analysed, it may be observed that the value of power loss due to oil splashing does not depend on power transmitted by the gear.

Oil kinematic viscosity  $v$  present in equations 16-18 is strongly dependent on oil temperature. Fig. 4 shows changes in oil kinematic viscosity  $v$  vs. oil temperature.

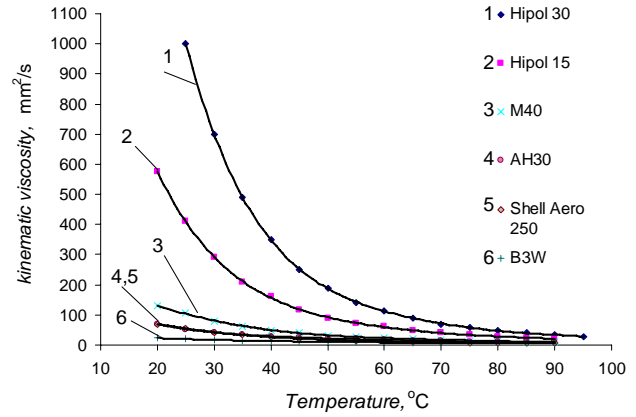


Fig. 4 Oil kinematic viscosity vs. oil temperature

To meet modelling requirements of oil temperature ranging from 20 to 90°C, the above relationships have been approximated with a polynomial (20). The coefficients for different oil types have been set out in Table. The type of polynomial approximation has been determined by best possible correlation with the data shown in Fig. 4.

$$v = a_0 + a_1 T + a_2 T^2 + a_3 T^3 + a_4 T^4 + a_5 T^5, \text{ mm}^2/\text{s} \quad (20)$$

where  $T$  is oil temperature (20-90°C);  $a_5 - a_0$  are polynomial coefficients as per Table.

The values of oil splashing power losses calculated with the help of above relationships are shown in

Table

Coefficients of polynomials approximating changes in oil kinematic viscosity

Oil type	$a_5$	$a_4$	$a_3$	$a_2$	$a_1$	$a_0$
Hipol 30	-1.76832801 e-06	+6.70219002 e-04	-1.02028855 e-01	+7.86486182 e+00	-3.11662203 e+02	+5.22577297 e+03
Hipol 15	-9.38461539 e-07	+3.31646749 e-04	-4.72559121 e-02	+3.43248607 e+00	-1.29732355 e+02	+2.12478280 e+03
M40	+1.69092641 e-07	-4.06445005 e-05	+2.93237418 e-03	+1.01777741 e-03	-8.28338295 e+00	+2.78297351 e+02
synthetic AH30	-1.48969755 e-07	+4.97296997 e-05	-6.55810205 e-03	+4.33061685 e-01	-1.49014273 e+01	+2.39679906 e+02
synthetic Shell Aero 250	+1.88959276 e-08	-3.69494901 e-07	-8.70578392 e-04	+1.32090211 e-01	-7.72735666 e+00	+1.78806695 e+02
synthetic B3W	-2.56578550 e-08	+7.48363824 e-06	-8.82214932 e-04	+5.57849825 e-02	-2.13194270 e+00	+4.90473399 e+01

Fig. 5. These values agree with those found experimentally, during gear operating at no-load and with different speeds. These tests have been carried out for a gear with circulating power, the test stand is shown in Fig. 6.

The test stand makes it possible for tested wheels to operate at different speeds and at loads controlled with torsional shafts, tightening coupling and lever with

weights. Two gears are included: one closing and one being tested, with identical transmission ratios and axle bases. The closing gear is driven by 15 kW electric motor via belt transmission.

Geometric parameters of the toothed wheels of the tested gear are:

- number of pinion teeth  $z_1 = 16$ ;

- number of gear teeth  $z_2 = 24$ ;
- gear ratio 1.5;
- helix angle  $\beta = 0$  degrees;
- face width  $b = 20$  mm;
- module pitch  $m_n = 4.5$  mm;
- coefficient of pinion addendum modification  $x_1 = 0.864$ ;
- coefficient of gear addendum modification  $x_2 = -0.5$ ;
- distance between the centres of the two gears 91.5 mm.

Wheel material: carburized steel 20H2N4A, hardened up to 60 HRC hardness.

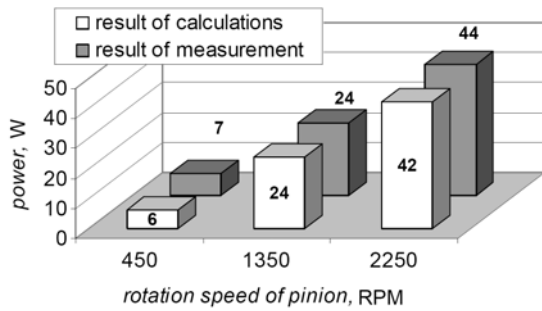
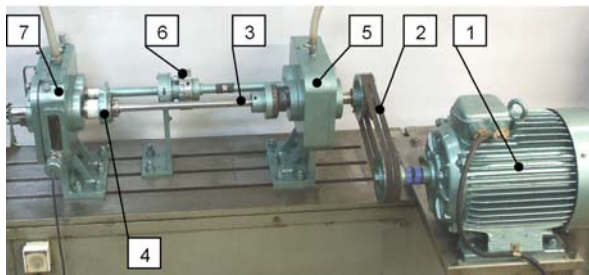
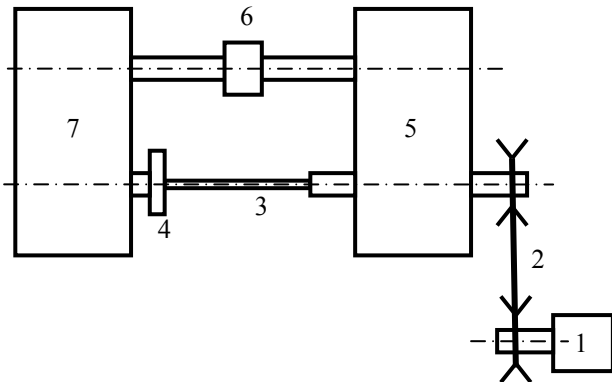


Fig. 5 Oil stirring power loss – test stand results



a



b

Fig. 6 Circulating power gear test stand: a – view of test rig, b – diagram, 1 - electric synchronous motor, 2 - belt transmission, 3 - torsional shaft, 4 - torque measuring clutch, 5 - closing gear, 6 - load clutch, 7 - tested gear

#### Determination of power losses at circulating power stand

The test stand (Fig. 6) with circulating power system has been used in the experiments. The power losses  $\Delta N$  have been determined in accordance with the heat bal-

ance method demonstrated in reference [15]; the gear has been additionally heated. This method utilises the relationship between gear temperature rise and power dissipated in the gear

$$Q = \text{const} \Delta t^{1.25} \quad (21)$$

where  $\Delta t$  is gear temperature rise relative to ambient temperature;  $Q$  is heating power.

Gear efficiency has been determined from the formula

$$\eta = \frac{N - \Delta N}{N} = 1 - \frac{\Delta N}{N} \quad (22)$$

where  $N$  is power transmitted by the gear;  $\Delta N$  is power losses corresponding to heating power.

#### 3.2. Bearing losses

In order to determine moment of friction of the bearings, the relationships presented in reference [30] have been used. The total bearing moment of friction is calculated as the sum of moment of friction independent of load  $M_0$  and moment of friction dependent on load  $M_1$

$$M_T = M_0 + M_1 \quad (23)$$

Moment of friction  $M_0$  depends on lubricant hydrodynamic losses, while moment  $M_1$  results from elastic strain and partial ball slip at the contact surface between rolling elements and bearing races.

#### 3.3. Losses caused by friction between teeth

The toothed gear efficiency values obtained by simulation (with teeth friction coefficient value assumed as in references [9, 29]) have been compared with the experimental test results obtained at circulating power test stand. These values were lower than experimental ones. Now, if we assume that modelling of the bearing losses demonstrated in section 2.2 in accordance with reference data does not require verification, the model is adapted in a different way; a new characteristic of meshing friction coefficient vs. linear meshing speed is calculated (Fig. 7). The obtained values of friction coefficient vary from 0.02 to 0.06 and correspond to the reference data.

The values of toothed gear efficiency computed by simulation have then been compared with the values

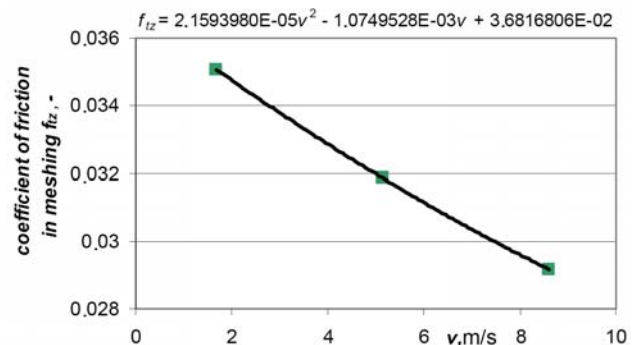


Fig. 7 Meshing friction coefficient vs. linear meshing speed – modified model

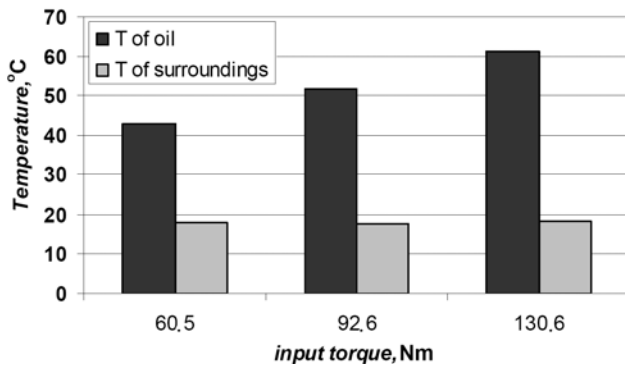


Fig. 8 Steady-state oil temperature and ambient temperature at pinion's rotational speed equal to 1350 rpm

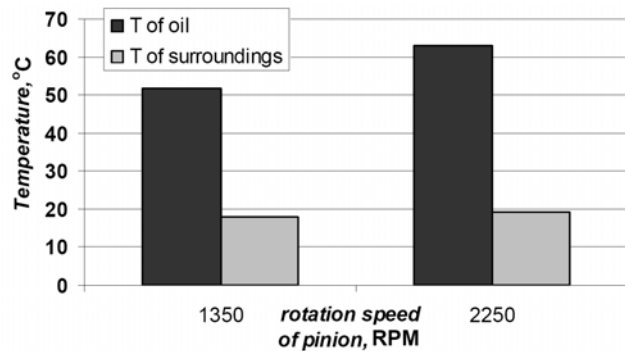


Fig. 9 Steady-state oil temperature and ambient temperature at input torque equal to 92.6 Nm

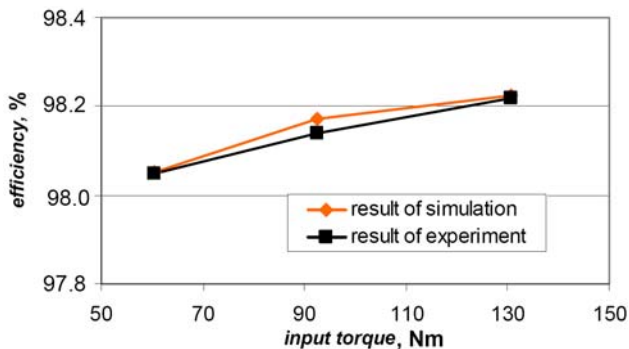


Fig. 10 Toothed gear efficiency vs. input torque at pinion's rotational speed equal to 1350 rpm – results of lab tests and computer simulations

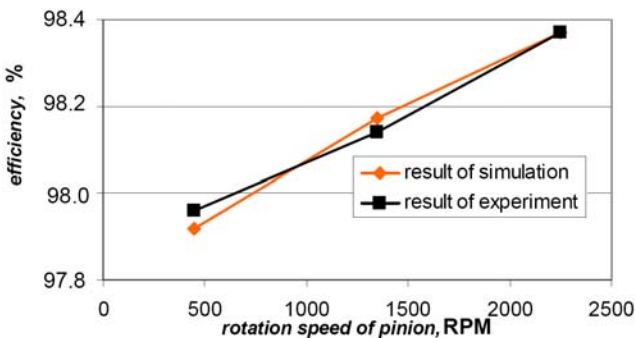


Fig. 11 Toothed gear efficiency vs. pinion's rotational speed at input torque equal to 92.6 Nm – results of lab tests and computer simulations

obtained by experiments carried out at the circulating power test stand. The comparison has been run for different gear loads and different pinion rotational speeds. The

computer simulations have been carried out taking into account oil temperature changes in gear due to load and rotational speed change (Figs. 8 and 9).

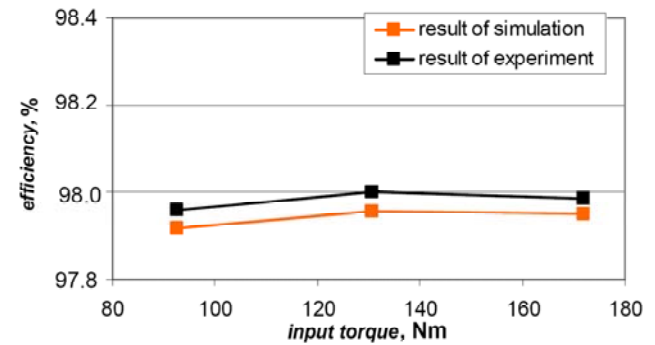


Fig. 12 Toothed gear efficiency vs. input torque at pinion's rotational speed equal to 450 rpm – results of lab tests and computer simulations

Figs. 10, 11 and 12 show the results of toothed gear efficiency computed by the simulation and obtained during laboratory tests at different rotational speeds and loads. The values are similar (comparable) and this fact proves that the used method of modelling toothed gear power losses is accurate. The achieved conformity of simulation and experimental research results has shown that application of an expanded and identified dynamic model of the gear in a power transmission system enables the acquisition of reliable diagnostic relations [31-40].

#### 4. Conclusions

1. The elaborated dynamic model of the drive system with toothed gear unites advantages of two modelling methods used previously. It takes into account principal links of drive kinematic chain such as electric drive motor, single-stage cylindrical gear, shaft coupling and process machine. At the same time, accurate description of dynamic phenomena taking place during wheel meshing, in accordance with modelling method proposed by L. Müller has been applied. This model has been implemented in Matlab-Simulink software environment.

2. To recapitulate the above results: it may be stated that gear oil temperature rise due to increase in transmitted power brings about decrease of power losses due to oil splashing. That is why during model investigation the changes of oil kinematic viscosity due to temperature must be taken into account.

3. Power losses due to friction between the teeth, bearing friction and oil splashing have been analyzed. Gear efficiency values obtained by numerical simulation and experimental tests for different rotational speeds and loads show satisfactory conformity.

#### References

1. **Vasylius, M., Didžiokas, R., Mažeika, P., Barzdaitis, V.** The rotating system vibration and diagnostics. -Mechanika. -Kaunas: Technologija, 2008, Nr.4(72), p.54-58.
2. **Antal, T.A.** A new algorithm for helical gear design with addendum modification. -Mechanika. -Kaunas: Technologija, 2009, Nr.3(77), p.53-57.

3. **Juzėnas, E., Jonuřas, R., Juzėnas, K.** Research of complex rotary systems vibrocondition based on analysis of dynamical processes and spectrum of vibrations. -Mechanika. -Kaunas: Technologija, 2008, Nr.1(69), p.42-45.
4. **Kovalev, N.A.** O dinamiczeskoj nagruzkie zubczatogo zaceplenia.-Mechanika i maszinostrojenije. -Izd. AN SSSR, OTN, 1960, No.2, p.10-29.
5. **Kovalev, N.A.** O maksimalnoj dinamiczeskoj nagruzke zubczatogo zaceplenia. -Maszinovedenie, 1965, No.5, p.12-30.
6. **Bollinger, J.G., Bosch, M.** Ursachen und Auswirkungen Dynamischer Zahnkrafte in Stirnradgetrieben. -Industrie Anzeiger, No.19/1964, p.319-326.
7. **Liu, G., Parker, R.G.** Impact of tooth friction and its bending effect on gear dynamics. -Journal of Sound and Vibration, 2009, 320, p.1039-1063.
8. **Rettig, H.** Innere dynamische Zusatzkrafte bei Zahnradgetrieben. -Antriebstechnik, 1977, No.11, p.655-663.
9. **Müller, L.** Gearbox Dynamics. -Warsaw: WNT, 1986. -167p. (in Polish).
10. **Nadolski, W.** Construction of mechanical models of some single-speed gearings in the case of torsional vibrations, Part 1. -Nonlinear Vibration Problems. -Warsaw: PWN, 1969, v.10, p.18-39.
11. **Nadolski, W.** Freedom torsional vibrations some n-stage gearing system. -The archive of mechanical engineering.-Warsaw, 1970, v.1, p.16-35 (in Polish).
12. **Pfeiffer, F. Kucukay, F.** Eine erweiterte mechanische Stosstheorie und ihre Anwendung in der Getriebedynamik. -VDI-Z, 1985, v.127, Nr.9, p.341-350.
13. **Litak, G. Friswell, M.I.** Vibration in gear systems. -Chaos, Solitons and Fractals 16, 2003, p.795-800.
14. **Radkowski, S.** Low-Energy Components of Vibroacoustics Signal as the Basis for Diagnosis of Defect Formation, -Machine Dynamics Problems.-Warsaw, 1995, v.12.-120p.
15. **Lazarz, B.** Identified dynamical model of toothed gear as the basis for design. -Katowice-Radom: ITE-PIB, 2001.-120p. (in Polish).
16. **Howard, J., Jia, S., Wang, J.** The dynamic modelling of a spur gear in mesh including friction and a crack. -Mechanical Systems and Signal Processing, 2001, 15(5), p.831-853.
17. **Andersson, A., Vedmar, L.** A dynamic model to determine vibrations in involute helical gears. -Journal of Sound and Vibration, 2003, 260, p.195-212.
18. **Cheng, Y., Lim, T.C.** Vibration analysis of hypoid transmissions applying an exact geometry-based gear mesh theory. -Journal of Sound and Vibration, 2001, 240(3), p.519-543.
19. **Sawalhi, N., Randall, R.B.** Simulating gear and bearing interactions in the presence of faults, Part I. The combined gear bearing dynamic model and the simulation of localised bearing faults. -Mechanical Systems and Signal Processing, 2008, 22, p.1924-1951.
20. **Endo, H.** A Study of Gear Faults by Simulation, and the Development of Differential Diagnostic Techniques. -Ph. D. Dissertation. -Sydney: UNSW, 2005. -178p.
21. **Bartelmus, W.** Mathematical modelling and computer simulations as an aid to gearbox diagnostics. -Mechanical Systems and Signal Processing, 2001, 15(5), p.855-871.
22. **Vonderschmidt, R.** Dynamische Zahnkräfte in Planetengetrieben. -Antriebstechnik, 1993, No.9, p.70-74.
23. **Taghirad H. D.** On the modeling and identification of harmonic drive systems, CIM Technical Report, CIM-TR-97-02, 1997.-78p.
24. **Özguven, H.N., Houser, D.R.** Mathematical models used in gear dynamics - a review. -Journal of Sound and Vibration, 1988, 121, p.383-411.
25. **Ryś, J.** Models of vibration and dynamic loads in toothed gears.-XVIII Symposium on Basic Machine Construction, Kielce-Ameliówka 16-20 september 1997, p.81-108 (in Polish).
26. Simulink Dynamic system Simulation for Matlab. Using Simulink version 3. -The Math Works, Inc., 1999. -210p.
27. **Dąbrowski, Z., Radkowski, S., Wilk, A.** Toothed gear dynamics – Investigation and simulation for exploitation oriented design. -Radom: ITE-PIB, 2000.-195p. (in Polish).
28. **Krzemiński - Freda, H.** Rolling Bearings. -Warsaw: PWN, 1985.-233p. (in Polish).
29. **Müller, L.** Gearbox Investigation. -Warsaw: WNT, 1984.-230p. (in Polish).
30. SKF General Catalog, Catalog 6000EN, 2005.-1129p.
31. **Wojnar, G.** Gear Fault Detection by Selected Methods of Vibration Signals Processing. Ph.D. thesis. -The Silesian University of Technology, Faculty of Transport, Department of Automotive Vehicle Construction, 2004. -187p. (in Polish).
32. **Sawalhi, N., Randall, R.B.** Simulating gear and bearing interactions in the presence of faults Part II: Simulation of the vibrations produced by extended bearing faults. -Mechanical Systems and Signal Processing, 2008, 22, p.1952-1966.
33. **Howard, I.** A review of rolling element bearing vibration: detection, diagnosis and prognosis. -DSTO-AMRL Report, DSTO-RR- 00113, 1994, p.35-41.
34. **Sopanen, J., Mikkola, A.** Dynamic model of a deep-groove ball bearing including localized and distributed defects. Part 1: Theory. -Proceedings of the Institution of Mechanical Engineers, vol. 217, Part K: J. Multi-body Dynamics, 2003, p.201-211.
35. **Stewart, R.M.** Some Useful Data Analysis Techniques For Gearbox Diagnostics, -Report MHM/R/10/77. -Machine Health Monitoring Group, Institute of Sound and Vibration Research, University of Southampton 1977.-19p.
36. **Madej, H., Lazarz, B., Wojnar, G.** Fault diagnosis in gears using WV distribution and wavelet analysis. -Inaugural World Congress on Engineering Asset Management Conrad Jupiters.-Gold Coast, Australia 11-14 July 2006, p.1-8.
37. **Decker, H.J.** Effects on Diagnostic Parameter after Removing Additional Synchronous Gear Meshes. -NASA/TM – 2003 – 212312 ARL- TR – 2933; 2003. -14p.
38. **Stander, C.J., Heyns, P.S.** Transmission path phase compensation for gear monitoring under fluctuating load conditions, -Mechanical Systems and Signal Processing, 2006, 20, p.1511-1522.
39. **Chen, P., Taniguchi, M., Toyota, T., He, Z.** Fault diagnosis method for machinery in unsteady operating

condition by instantaneous power spectrum and genetic programming, -Mechanical Systems and Signal Processing, 2005, 19, p.175-194.

40. **Czech, P., Łazarz, B., Wojnar, G.** Detection of Local Gears Tooth Faults by Using Artificial Neural Networks and Genetic Algorithm. -Katowice-Radom: ITE-PIB, 2007.-199p. (in Polish).

B. Łazarz, G. Wojnar, H. Madej, P. Czech

#### EKSPERIMENTINIS IR ANALITINIS NUOSTOLIŲ KRUMPLINĖJE PAVAROJE NUSTATYMAS

##### R e z i u m ė

Straipsnyje, naudojantis Matlab-Simulink programine įranga, tyrinėjamas krumplinės pavaros dinaminis modelis. Atlikus modelio dinaminę analizę, projektavimą ir techninę diagnostiką, gautus duomenis reikia patikrinti. Vienas iš tikrinamų modelio parametrų yra perdavimo jėgos nuostoliai sistemoje. Tai turi įtakos krumplinės pavaros naudingumo koeficientui. Jėgos nuostoliai krumplinėje pavaroje susidaro dėl dantų susikabinime atsirandančios trinties jėgos bei tepimo proceso. Jėgos nuostolių įvertinimas turi didelę įtaką lyginant tarpusavyje analitinius skaičiavimus ir eksperimentiškai gautus rezultatus. Straipsnyje tyrinėjamas jėgos pavaroje netekimas dėl trinties, atsirandančios dantų susikabinime, guoliuose ir dėl tepalo taškymo. Krumplinės pavaros efektyvumas, apskaičiuotas esant skirtingiems pavaros sukimosi greičiams bei apkrovoms ir nustatytas eksperimentiškai, sutapo gana gerai.

B. Łazarz, G. Wojnar, H. Madej, P. Czech

#### EVALUATION OF GEAR POWER LOSSES FROM EXPERIMENTAL TEST DATA AND ANALYTICAL METHODS

##### S u m m a r y

This paper deals with Matlab-Simulink mathematical model of power transmission systems with toothed gear. If this model is to be used in dynamic analysis, design and technical diagnostics, then its parameters must be

verified. One of these parameters is power loss coefficient which has influence on gear efficiency. Power losses in gears come mainly from the friction between the teeth and lubrication process during the meshing. Evaluation of gear power losses has a significant influence on the agreement between numerical and experimental results obtained from test stand. Power losses due to friction between the teeth, bearing friction and oil splashing have been analyzed in the paper. Gear efficiency values obtained by numerical simulation and experimental tests for different rotational speeds and loads show satisfactory conformity.

Б. Лазарс, Г. Войнар, Г. Мадей, Р. Чех

#### ОПРЕДЕЛЕНИЕ ПОТЕРЬ МОЩНОСТИ В ЗУБЧАТОМ ЗАЦЕПЛЕНИИ НА ОСНОВЕ ЭКСПЕРИМЕНТАЛЬНЫХ ДАННЫХ И АНАЛИТИЧЕСКОГО РАСЧЕТА

##### Р е з ю м е

В статье представлена динамическая модель привода с зубчатой передачей, анализируемая в среде Matlab-Simulink. Использование указанной модели при динамическом анализе, проектировании и технической диагностике требует верификации параметров модели. Одним из таких параметров является коэффициент потери мощности, который оказывает влияние на КПД передачи. В зубчатых передачах потери мощности связаны в основном с трением между зубами и процессом смазки. Определение потери мощности имеет существенное влияние на полученные результаты моделирования и их качественное и количественное соответствие экспериментальным данным. В статье исследуются потери мощности из-за трения между зубами, трения в подшипниках и разбрызгивания масла. Эффективность зубчатой передачи установлена при различных скоростях вращения и нагрузках. Совпадение результатов, полученных при численном моделировании и экспериментальных исследованиях удовлетворительное.

Received August 18, 2009

Accepted December 01, 2009

DOI: 10.5755/j02.mech.15501